RSC Advances

PAPER

View Article Online
View Journal | View Issue



Cite this: *RSC Adv.*, 2017, **7**, 36852

# Enhanced hydrogen storage properties of a dual-cation ($Li^+$, $Mg^{2+}$) borohydride and its dehydrogenation mechanism†

Liuting Zhang,‡[ab] Jiaguang Zheng,‡[ac] Xuezhang Xiao,*[a] Xiulin Fan,[d] Xu Huang,[a] Xinlin Yang[b] and Lixin Chen*[ac]

Received 13th June 2017
Accepted 21st July 2017

DOI: 10.1039/c7ra06599j

rsc.li/rsc-advances

In this paper, we present a new method to synthesize a dual-cation ($Li^+$, $Mg^{2+}$) borohydride. It is found that Li–Mg–B–H is formed by mechanical milling a mixture of $LiBH_4$ and $MgCl_2$ with a molar ratio of 3 : 1 in diethyl ether ($Et_2O$) and a subsequent heating process. The morphology and structure of the as-prepared Li–Mg–B–H compound are studied by SEM, XRD, FTIR and NMR measurements. Further experiments testify that Li–Mg–B–H can release approximately 12.3 wt% of hydrogen under 4 bar initial hydrogen pressure from room temperature to 500 °C and reach a maximum desorption rate of 13.80 wt% per h at 375 °C, which is 30 times faster than that of pristine $LiBH_4$. Thermal analysis indicates that the decomposition process of the new compound involves three steps: (1) Li–Mg–B–H first decomposes into $LiBH_4$ and $MgH_2$ and synchronously releases a number of $H_2$ molecules; (2) $MgH_2$ decomposes to Mg and $H_2$; (3) $LiBH_4$ reacts with Mg, generating $H_2$, $MgB_2$ and LiH. Moreover, Li–Mg–B–H is proved to be partially reversible, which can release 5.3 wt% hydrogen in the second dehydrogenation process. The strategy of altering the $\chi_p$ of metal ions in borohydrides may shed light on designing dual-cation borohydrides with better hydrogen storage performance.



## Introduction

Hydrogen, which produces nearly zero pollutant emission from power generators, is regarded as one of the most promising cost-effective and renewable energy carriers during past decades. However, a safe hydrogen storage technology with a high energy density still challenges scientists worldwide.[1,2] $LiBH_4$, which has high gravimetric and volumetric hydrogen densities (18.5 wt% and 121 kg·$H_2$ per $m^3$), is regarded as one of the most promising hydrogen storage materials.[3,4] Nevertheless, $LiBH_4$ is thermodynamically stable and kinetically sluggish in dehydrogenation. Besides, extremely rigorous temperature and pressure conditions are required for $LiBH_4$ to re-form, which severely limits its practical on-board automobile application.

In past decades, numerous attempts have been carried out to destabilize $LiBH_4$, including catalyst doping,[5–10] reactive composite formation,[11–16] nanoconfinement[17,18] and a combination of strategies.[19–26] Recently, Orimo *et al.* found that the thermodynamic stability of ionic borohydrides can be correlated fairly well with the Pauling electronegativity $\chi_p$ of metal ions, $M^{n+}$; the higher $\chi_p$ of $M^{n+}$, the less stable $M(BH_4)_n$ will be.[27,28] This finding suggests that the thermodynamic stability of $LiBH_4$ can be tuned by using metal ions $M^{n+}$ with higher $\chi_p$ to partially substitute the Li cations to form a dual-cation borohydride $LiM(BH_4)_{n+1}$. Employment of this strategy has yielded several novel dual-cation borohydrides. Jiang *et al.*[29] successfully synthesized a new Li–Ca–B–H complex borohydride with its first dehydrogenation step started at *ca.*70 °C, much lower than those of pristine $LiBH_4$ and $Ca(BH_4)_2$. Choudhury *et al.*[26] prepared a new complex hydride $LiMn(BH_4)_3$ with a 3 : 1 ratio of precursor materials $LiBH_4$ and $MnCl_2$ *via* the solid-state mechano-chemical process. Thermogravimetric analysis (TGA) of $LiMn(BH_4)_3$ indicated that *ca.* 8.0 wt% hydrogen can be released between 135 °C and 155 °C in a single dehydrogenation step. Kim *et al.*[30] found that ball milling $LiBH_4$ and $ScCl_3$ produced LiCl and a unique crystalline hydride, which has been unequivocally identified *via* multinuclear solid-state nuclear magnetic resonance (NMR) to be $LiSc(BH_4)_4$. Fang *et al.*[31] claimed that they had synthesized a dual-cation borohydride directly from $LiBH_4$ and $Mg(BH_4)_2$ with molar ratio of 1 : 1. Rapid hydrogen release from the $LiBH_4/Mg(BH_4)_2$ sample was

[a]*State Key Laboratory of Silicon Materials, School of Materials Science and Engineering, Zhejiang University, Hangzhou 310027, P.R. China. E-mail: xzxiao@zju.edu.cn; lxchen@zju.edu.cn; Fax: +86 571 87951152; Tel: +86 571 87951152*

[b]*School of Energy and Power, Jiangsu University of Science and Technology, Zhenjiang 212003, P.R. China*

[c]*Key Laboratory of Advanced Materials and Applications for Batteries of Zhejiang Province, Hangzhou 310013, P.R. China*

[d]*Department of Chemical and Biomolecular Engineering, University of Maryland, College Park, MD 20742, USA*

† Electronic supplementary information (ESI) available. See DOI: 10.1039/c7ra06599j

‡ Liuting Zhang and Jiaguang Zheng contributed equally.

initiated at around 240 °C, which is about 30 °C and 170 °C lower than that of $LiBH_4$ and $Mg(BH_4)_2$. However, Bardají *et al.*[32] investigated the physical mixture of $xLiBH_{4(1-x)}Mg(BH_4)_2$ with $x = 0, 0.10, 0.25, 0.33, 0.40, 0.50, 0.60, 0.66, 0.75, 0.80, 0.90, 1$ and found it was only a physical mixture but not a dual-cation borohydride. The eutectic composition was found to exist at $0.50 < x < 0.60$ exhibiting a eutectic melting at 180 °C and the decomposition of the material begins right after the melting. At 270 °C the $x = 0.50$ composite release about 7.0 wt% of hydrogen. Therefore no confirmed synthesis of dual-cation $LiMg(BH_4)_3$ has been reported yet.

Inspired by the theory and experiments above, it seems that thermodynamic stability of $LiBH_4$ can be decreased by introducing metal ions with higher $\chi_p$. Besides, the most feasible way to synthesize a dual-cation borohydride is milling $LiBH_4$ with metal chloride. In this paper, we focus on the Li–Mg–B–H system, aiming to elucidate the possible formation of a dual-cation borohydride *via* wet-milling $LiBH_4$ and $MgCl_2$ in $Et_2O$. The samples are carefully characterized and determined by the SEM, XRD, FTIR and NMR measurements, and their hydrogen storage properties have been investigated.

## Experimental section

All sample operations were performed in an Ar-filled glovebox, which was equipped with a circulative purification system to maintain the $H_2O$ and $O_2$ levels below 0.1 ppm. $LiBH_4$ (assay 95%, Alfa Aesar), $NaBH_4$ (96%, Sinopharm Chemical Reagent co., Ltd) and $MgCl_2$ (assay 98%, Sigma) were used as starting materials. $Et_2O$ ($C_4H_{10}$, 99.5%, Hangzhou Chemical Reagent co., Ltd) was used as solvent. 2 g mixture of $LiBH_4$ and $MgCl_2$ in a molar ratio of 3 : 1 together with 60 mL of $Et_2O$ was put into a stainless steel vial with a ball-to-power ratio of 20 : 1. The ball milling process was carried out on a planetary ball mill (QM-3SP4, Nanjing, China) under 1 MPa high purity $H_2$ (99.999%) at a speed of 400 rpm. The milling process was paused 0.1 h for every 0.4 h to avoid the increase of temperature. The prepared liquid mixture flowed through a homemade filtration device to remove the by-product LiCl. Then the filtered liquid was heated to 205 °C in a homemade vial and vacuumed at the same time for 2 h to eliminate the solvent, and the dry products were obtained. In comparison, $Mg(BH_4)_2$ was synthesized from $MgCl_2$ and $NaBH_4$ in dried diethyl ether as described previously.[33]

Differential scanning calorimetry (DSC) measurements were conducted on a Netzsch STA 449 F3 analyzer under high purity flowing argon conditions (99.999%, 50 mL $min^{-1}$). The hydrogen desorption/absorption properties were quantitatively evaluated by a volumetric method on a Sieverts-type apparatus, where the experimental data were monitored and recorded automatically. About 150 mg of sample was used for each temperature programmed desorption (TPD) measurement. In the temperature ramp experiments, the temperature was gradually elevated from room temperature to 500 °C at a heating rate of 2 °C $min^{-1}$ for dehydrogenation (under 4 bar initial hydrogen pressure) and hydrogenation (initially hydrogen pressure being 100 bar). For isothermal examination, the sample was heated to a desired temperature rapidly and kept during the entire measurement.

Morphology and elemental distribution of samples were identified by scanning electron microscopy (SEM, Hitachi SU-70) equipped with an energy dispersive X-ray spectroscopy (EDX, HORIBAX-Max). X-ray diffraction analysis was conducted on an X'Pert Pro X-ray diffractometer (PANalytical, Netherlands) with Cu Kα radiation at 40 kV and 40 mA. A special container fully filled with high purity Ar was prepared to avoid air exposure during sample transferring and testing. Fourier transform infrared (FTIR) spectra were obtained with a Bruker Tensor 27 unit in transmission mode. Solid state magic angle spinning (MAS) NMR spectra were obtained using a Bruker Avance 300 MHz spectrometer with a wide bore 7.04 T magnet and employing a boron-free Bruker 7 mm CPMAS probe. The spectral frequency was 75 MHz for the $^{11}B$ nucleus and the NMR shifts are reported in parts per million (ppm) externally referenced to $NaBH_4$. The powder materials were packed into 7 mm $ZrO_2$ rotors in an argon-filled glovebox and were sealed with tight fitting Kel-F caps. The one-dimensional (1D) $^{11}B$ MAS NMR spectra were acquired after a 1.7 μs single π/2 pulse (corresponding to radio field strength of 92.6 kHz). The spectra were recorded at a MAS spinning rate of 5 kHz. The recovery delay was set to 5 s. Spectra were acquired at 20 °C.

## Results and discussion

### Morphology and structure of as-prepared samples

SEM images of as-prepared samples are presented in Fig. 1. $LiBH_4$ has a flocculent surface in Fig. 1a (×1.00k) and larger magnification picture (Fig. 1b) shows a smooth surface with small holes in it. Comparing Fig. 1c with 1e, the as-synthesized $Mg(BH_4)_2$ presents similar morphology with the as-prepared Li–Mg–B–H but with worse electroconductivity. Under enlarged magnification, as-prepared Li–Mg–B–H shows a smooth surface similar to that of $LiBH_4$, while a much rougher surface with small particles on it emerges in the as-synthesized $Mg(BH_4)_2$. In addition, as we can see from the EDX mapping data of Li–Mg–B–H in Fig. S1,† the Mg and B elements are dispersed homogeneously in the Li–Mg–B–H matrix, further demonstrating the possibility of the formation of a new compound.

In order to determine the microstructures of as-prepared Li–Mg–B–H, XRD and FTIR examinations of $LiBH_4$, as-synthesized $Mg(BH_4)_2$ and as-prepared Li–Mg–B–H were recorded, presented in Fig. 2. The XRD pattern of as-synthesized $Mg(BH_4)_2$ in Fig. 2c shows diffraction peaks of both low temperature phase α-$Mg(BH_4)_2$ and high temperature phase β-$Mg(BH_4)_2$,[34] indicating that the as-synthesized $Mg(BH_4)_2$ was a mixture of α-$Mg(BH_4)_2$ and β-$Mg(BH_4)_2$. The physical mixture of $LiBH_4$ and $Mg(BH_4)_2$ with a molar ratio of 1 : 1 (Fig. 2e) shows the total diffraction peaks of $LiBH_4$ and $Mg(BH_4)_2$. The appearance of LiCl in Fig. 2d and in the filter residue (Fig. S2†) demonstrates the reaction between $LiBH_4$ and $MgCl_2$ occurred during the wet-chemical ball milling process. Combining all the analyses of the diffraction patterns of relevant samples, peaks at $2\theta = 16°$, 18.1°, 19.1°, 25°, 27.3° in Fig. 2d should be assigned predominately to a new phase, this agrees well with Fang's[31] conclusion and these new phases may come from a new dual-cation borohydride.

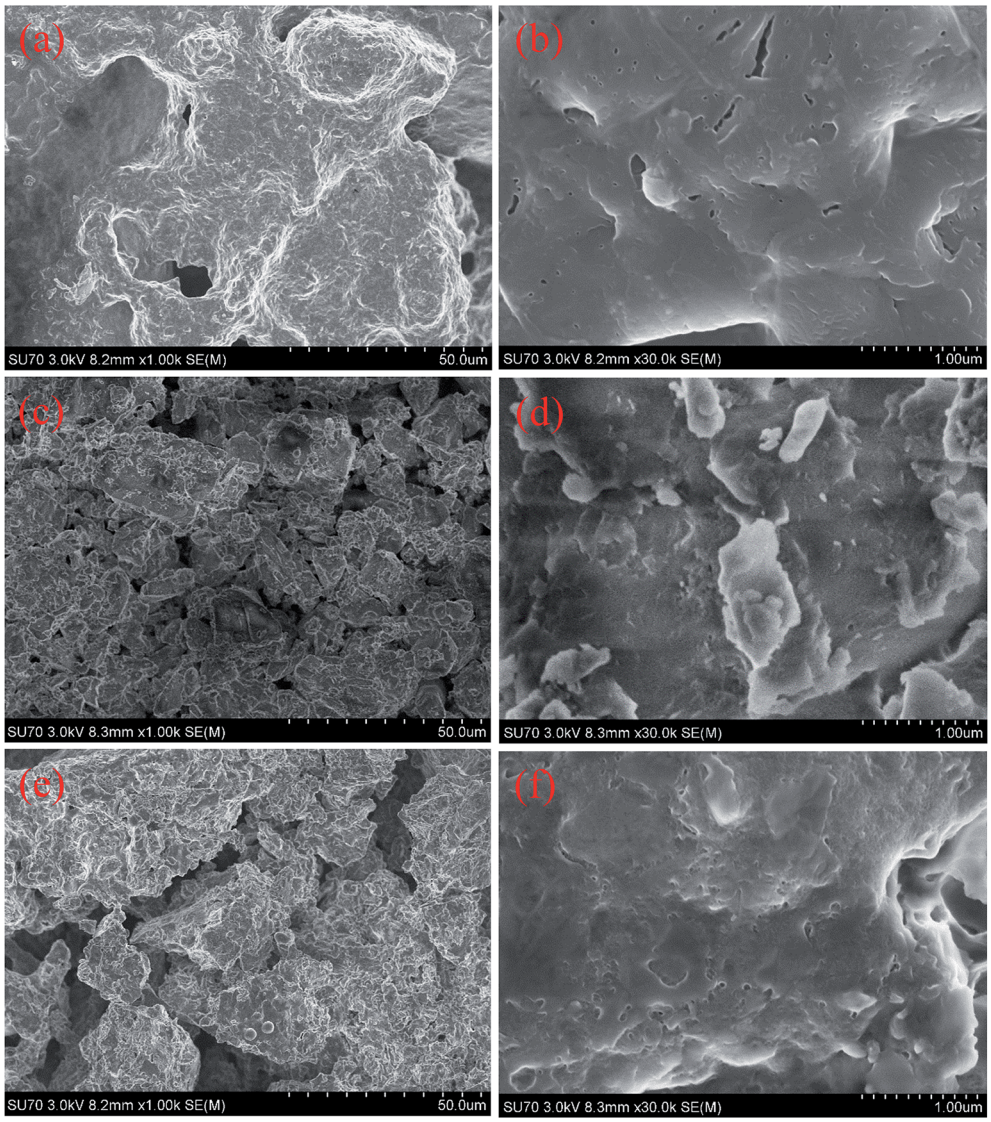


Fig. 1 SEM images of (a, b) $LiBH_4$, (c, d) as-synthesized $Mg(BH_4)_2$ and (e, f) as-prepared Li–Mg–B–H.

From the results of FTIR measurements, typical features of $[BH_4]^{1-}$ group can be readily observed in the spectra, *i.e.* the stretching and deformation of B–H bonds in the regions between 2200 and 2400 $cm^{-1}$ and 1100 and 1300 $cm^{-1}$, respectively.[3] The B–H absorption band is split into three contributions at 2386 $cm^{-1}$, 2291 $cm^{-1}$, and 2223 $cm^{-1}$. The B–H bending vibration in $LiBH_4$ is at 1125 $cm^{-1}$ while that of $Mg(BH_4)_2$ is split into two contributions at 1125 $cm^{-1}$ and 1267 $cm^{-1}$. The presence of an absorption band around 1033 $cm^{-1}$ contributes to $\alpha$-$Mg(BH_4)_2$.[34] Furthermore, the absorption band in the regions between 650 and 700 $cm^{-1}$ originate from $Mg(BH_4)_2$. The mixed $LiBH_4$ and $Mg(BH_4)_2$ shows all the bands of $LiBH_4$ and $Mg(BH_4)_2$, as displayed in Fig. 2e. Combining the above analysis, we can see that as-prepared Li–Mg–B–H sample shares the same stretching and deformation of B–H bonds with physically combined $LiBH_4$–$Mg(BH_4)_2$ but also has slight difference. It does not show the absorption band in the regions between 650 and 700 $cm^{-1}$, which originate from $Mg(BH_4)_2$.

In order to further clarify the specificity of Li–Mg–B–H, NMR measurements were adopted to test the chemical shift of $^{11}B$ of $LiBH_4$, as-synthesized $Mg(BH_4)_2$, as-prepared Li–Mg–B–H, physical mixed $LiBH_4$–$Mg(BH_4)_2$, respectively. If the as-prepared Li–Mg–B–H is a physical mixture, the chemical shift peak of $^{11}B$ should be a combination of those of $LiBH_4$ and $Mg(BH_4)_2$. However, as the NMR results shown in Fig. 3, as-prepared Li–Mg–B–H exhibits different peaks. The peaks of $LiBH_4$, $Mg(BH_4)_2$ and physical mixed $LiBH_4$–$Mg(BH_4)_2$ appear at −40.30, −39.89, and −40.02 ppm, respectively. The peak of physical mixed sample is asymmetric (a shoulder at around −45 ppm) and the chemical shift is just between −40.30 and-39.89 ppm, which proves the nature of physical mixing. However, the chemical shift of $^{11}B$ in the primary new Li–Mg–B–H compound is −39.59 ppm, indicating a new chemical circumstance for B. Considering that the starting ingredient are $3LiBH_4$–$MgCl_2$, the new compound is more likely to be $LiMg(BH_4)_3$. Due to the limitation of laboratory equipment, currently we cannot

 

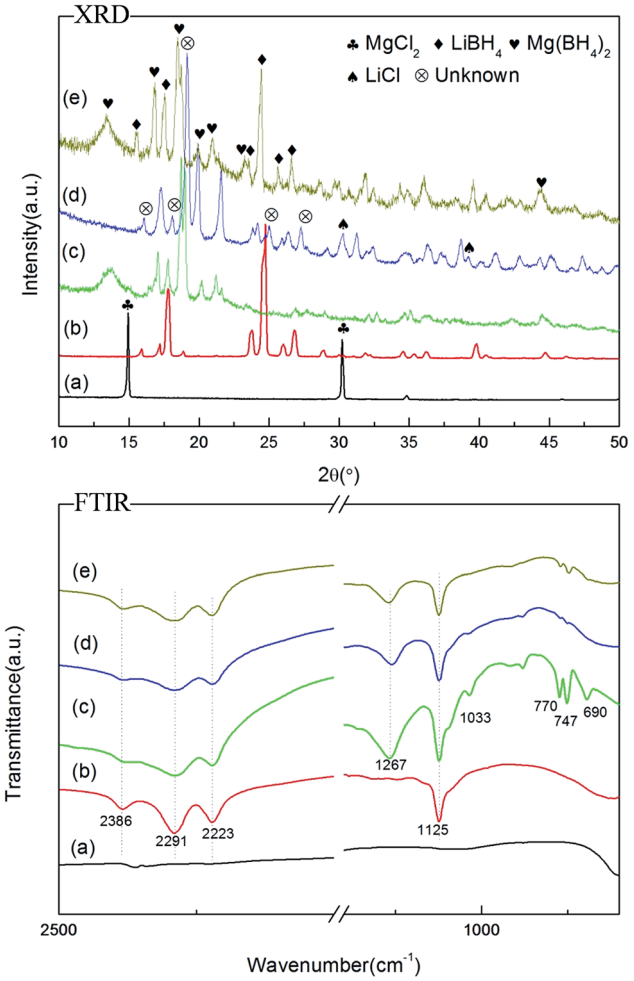


Fig. 2 XRD patterns and FTIR spectra of (a) $MgCl_2$, (b) $LiBH_4$, (c) as-synthesized $Mg(BH_4)_2$, (d) as-prepared Li–Mg–B–H, (e) physical mixed $LiBH_4$–$Mg(BH_4)_2$.

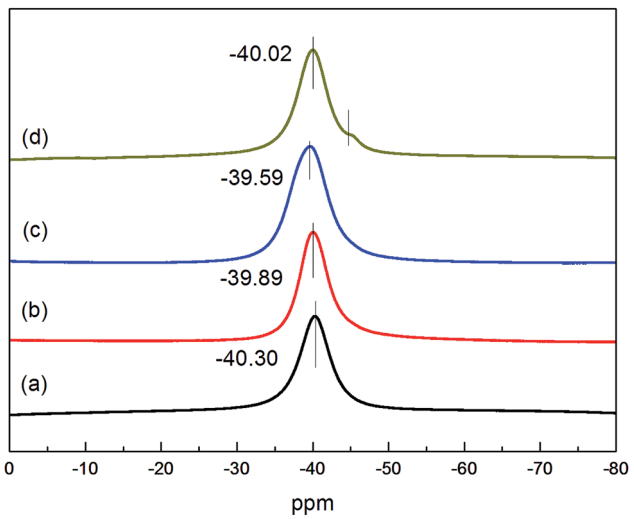


Fig. 3 $^{11}B$ MAS NMR spectra of the (a) $LiBH_4$, (b) as-synthesized $Mg(BH_4)_2$, (c) as-prepared Li–Mg–B–H, (d) physical mixed $LiBH_4$–$Mg(BH_4)_2$.

measure out the exact composition of the new compound. Through the above discussion, the as-prepared Li–Mg–B–H is not just a physical mixture of $LiBH_4$ and $Mg(BH_4)_2$ but a new dual-cation borohydride.

## Hydrogen desorption performance

The DSC-MS characteristics of as-prepared Li–Mg–B–H are shown in Fig. 4. DSC curve exhibits five endothermic peaks, which correspond to the structure transition (104.4 °C), melting (174.2 °C), and decomposition of as-prepared Li–Mg–B–H (260.9, 358.3, 391.6 °C), respectively.[12] MS results demonstrate that the gas released is pure $H_2$ without $B_2H_6$, and MS desorption peak temperatures are in good agreement with DSC results. Kou *et al.*[35] found that initial hydrogen pressure had a great impact on the dehydrogenation of $2LiBH_4$–$MgH_2$ system. Under four bar initial hydrogen pressure, $LiBH_4$ reacts with Mg to yield $MgB_2$, which is essential for the reversibility of this system. Four bar initial hydrogen pressure was also adopted to explore its effect on the decomposition of Li–Mg–B–H. Fig. S3† presents the XRD patterns of the decomposed sample of Li–Mg–B–H at different initial hydrogen pressures. We can see from Fig. S3† that when hydrogen pressure raises to 4 bar a tip bumps up at around 42°, which is the main diffraction peak of $MgB_2$. This testifies that four bar initial hydrogen pressure can help to form $MgB_2$ during decomposition. Hence, variable temperature hydrogen desorption behavior of the as-prepared samples was conducted using a TPD apparatus under four bar initial hydrogen pressure.

Fig. 5 shows TPD curves of $LiBH_4$, as-synthesized $Mg(BH_4)_2$ and as-prepared Li–Mg–B–H. It was observed that the decomposition of the pristine $LiBH_4$ started sluggishly at 320 °C, resulting in a final release of 4.3 wt% hydrogen at 500 °C. As-synthesized $Mg(BH_4)_2$ first decomposed at 300 °C, quickly releasing a large amount of $H_2$ with the elevating temperature and finally reached a 11.7 wt% hydrogen release at 500 °C. Worth-noting, the operating temperature for hydrogen desorption of as-prepared Li–Mg–B–H was significantly reduced to 250 °C, 70 °C and 50 °C lower compared to that of pristine $LiBH_4$ and as-synthesized $Mg(BH_4)_2$, respectively. In total, 12.3 wt% hydrogen was released from the dual-cation borohydride, which is three times larger comparing to that of pristine $LiBH_4$ (4.3 wt%) and higher than that of as-synthesized $Mg(BH_4)_2$ (11.7 wt%). Furthermore, the new compound can release hydrogen at a rate of 13.80 wt% per h at 375 °C, just as fast as as-synthesized $Mg(BH_4)_2$, 30 times faster than pristine $LiBH_4$ (0.45 wt% per h). The findings indicate that the idea of using higher $\chi_p$ of metal ions $Mg^{2+}$ to partially substitute the Li cations to form a dual-cation borohydride Li–Mg–B–H truly improves both the dehydrogenation thermodynamics and kinetics of $LiBH_4$.

## Dehydrogenation reaction mechanism

In order to fully understand the dehydrogenation process, the as-prepared Li–Mg–B–H was heated to different temperatures (295, 395, and 495 °C) according to the DSC-MS and TPD results and the decomposed products were collected and applied with XRD and FTIR measurements, displayed in Fig. 6. In the XRD

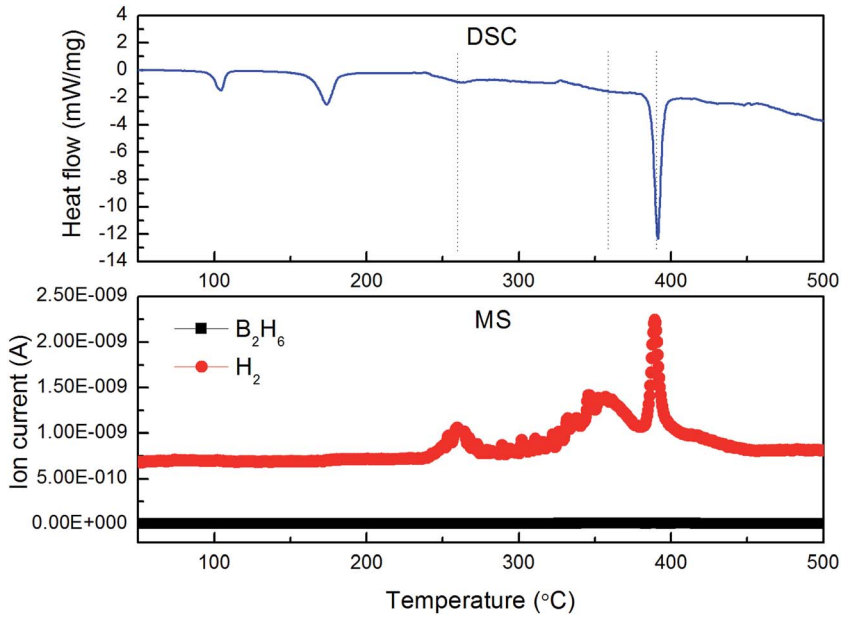


Fig. 4 DSC and MS profiles of Li–Mg–B–H at a heating rate of 5 °C $min^{-1}$ from room temperature to 500 °C.

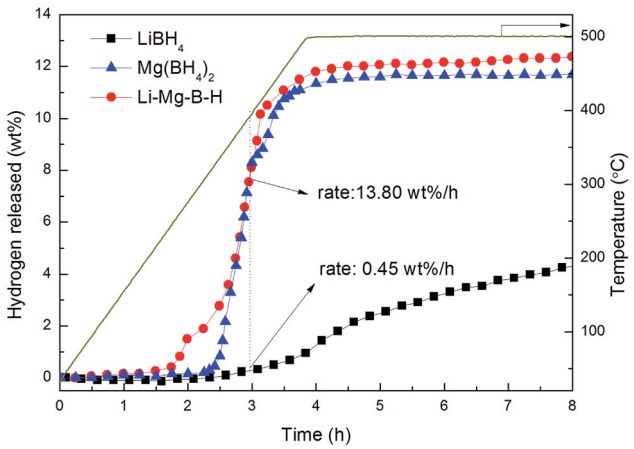


Fig. 5 TPD profiles of $LiBH_4$, $Mg(BH_4)_2$ and Li–Mg–B–H at a heating rate of 2 °C $min^{-1}$ from room temperature to 500 °C under 4 bar initial hydrogen pressure.

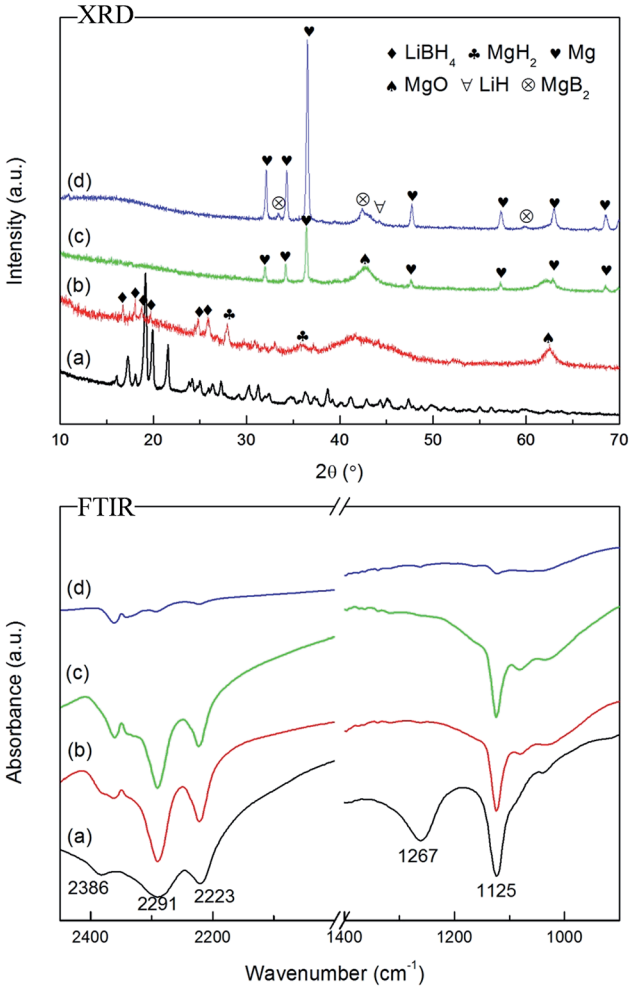


Fig. 6 XRD patterns and FTIR spectra of Li–Mg–B–H decomposed at different temperatures: (a) room temperature, (b) 295 °C, (c) 395 °C, and (d) 495 °C.

patterns, Fig. 6b shows that high-temperature phase of $LiBH_4$, $MgH_2$ and MgO (MgO comes from the air contamination of the sample during operation) formed after heated at 295 °C. From the FTIR profile in Fig. 6b, we can see that the peaks of the B–H bonding at 2291, 2223 and 1125 $cm^{-1}$, which confirm the presence of $LiBH_4$.[6] When heated up to 395 °C, metallic Mg and MgO are the only phases detected by XRD, whereas the diffraction peaks of $MgH_2$ are completely absent. The FTIR pattern shows that $LiBH_4$ still exists. So in this step, $MgH_2$ decomposes to Mg and $H_2$. As the dehydrogenation temperature further increases to 495 °C, the final products are Mg, MgO, $MgB_2$ and LiH. And the peaks of B–H bonds disappear in FTIR, indicating the complete decomposition of $LiBH_4$. To sum up, the main decomposition pathway of the new compound under four bar initial hydrogen pressure can be described as follows:

(Step 1)

$$\text{Li–Mg–B–H} \rightarrow x\text{LiBH}_4 + \text{MgH}_2 + \text{B} + \text{H}_2\ (0 < x \leq 1)$$

(Step 2)

$$\text{MgH}_2 \rightarrow \text{Mg} + \text{H}_2$$

(Step 3)

$$x\text{LiBH}_4 + \text{Mg} \rightarrow 0.5x\text{MgB}_2 + x\text{LiH} + 1.5x\text{H}_2 + (1 - 0.5x)\text{Mg}$$

### Hydrogen storage reversibility

Reversibility is one of the key features for hydrogen storage materials, especially for on-board applications. In order to study the reversibility of the new compound, we use temperature programmed absorption as well as isothermal rehydrogenation. Fig. 7a shows the temperature absorption curve from room temperature to 500 °C with a heating rate of 2 °C $min^{-1}$. The pressure is increasing linearly before the temperature is heated to 420 °C, while maintaining and even decreasing when the temperature is above 420 °C. This indicates that the

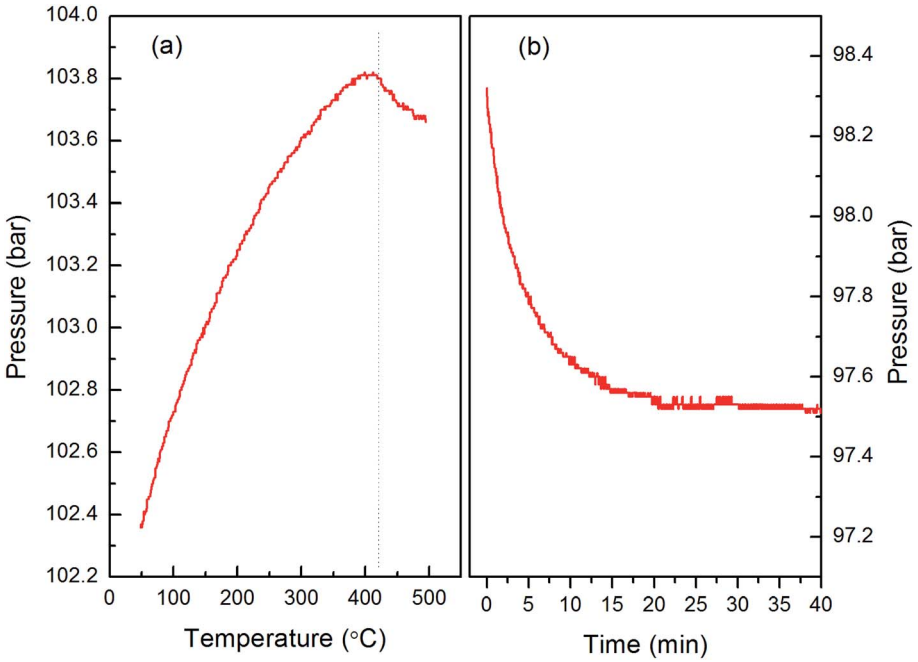


Fig. 7 The rehydrogenation curves of the dehydrogenated sample of Li–Mg–B–H: (a) temperature programmed absorption from room temperature to 500 °C at a heating rate of 2 °C $min^{-1}$ and (b) isothermal rehydrogenation at 420 °C.

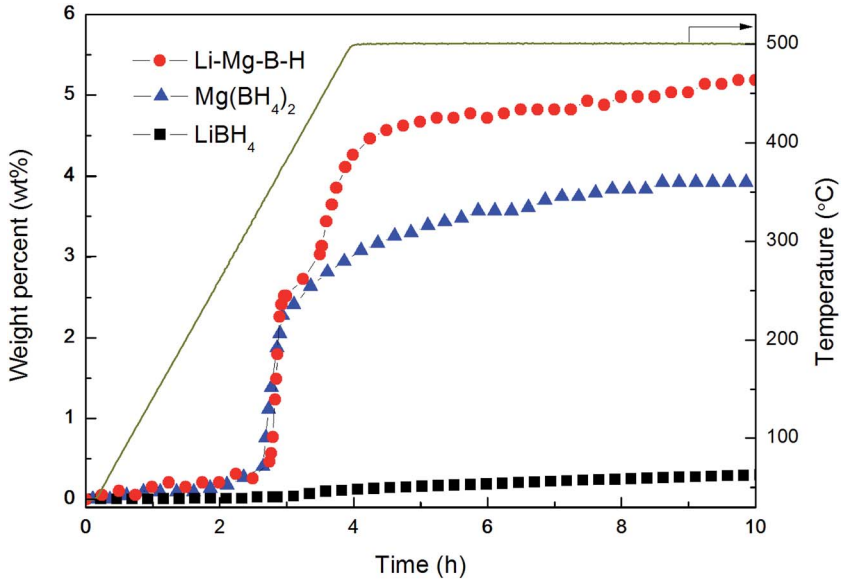


Fig. 8 Hydrogen desorption curve at a heating rate of 2 °C $min^{-1}$ of the rehydrogenated sample.

dehydrogenated product of Li–Mg–B–H could be rehydrogenated at about 420 °C. From the isothermal rehydrogenation curve at 420 °C in Fig. 7b, the reduction in hydrogen pressure is related to the amount of absorbed hydrogen. XRD patterns (see in Fig. S4†) show that the rehydrogenated sample is composed of $MgH_2$ and $LiBH_4$. The dehydrogenation performance of the rehydrogenated sample was further carried out. The dehydrogenation curve is shown in Fig. 8, and it can be observed that the rehydrogenated products can release 5.3 wt% hydrogen, indicating that the new compound has certain reversibility. Nevertheless, this is a great improvement for the reversibility of Li–Mg–B–H comparing with a previous work,[31] which can only be rehydrogenated to $MgH_2$ and release about 2 wt% hydrogen. Owing to the complexity of Li–Mg–B–H, detailed experimental and theoretical studies are still required to better understand the cyclic de/rehydrogenation behaviors of the Li–Mg–B–H system.

## Conclusion

In summary, a new dual-cation borohydride Li–Mg–B–H has been successfully synthesized by ball-milling $3LiBH_4 + MgCl_2$ mixture in $Et_2O$. Further investigations show that dehydrogenation performance of the new Li–Mg–B–H was affected by initial hydrogen pressure. Under four bar initial hydrogen pressure, the onset dehydrogenation temperature of Li–Mg–B–H (250 °C) is 70 °C and 50 °C lower compared to pristine $LiBH_4$ and $Mg(BH_4)_2$, respectively. The Li–Mg–B–H can release 12.3 wt% hydrogen from room temperature to 500 °C according to the following three steps:

(Step 1)

$$\text{Li–Mg–B–H} \rightarrow x\text{LiBH}_4 + \text{MgH}_2 + \text{B} + \text{H}_2\ (0 < x \leq 1)$$

(Step 2)

$$\text{MgH}_2 \rightarrow \text{Mg} + \text{H}_2$$

(Step 3)

$$x\text{LiBH}_4 + \text{Mg} \rightarrow 0.5x\text{MgB}_2 + x\text{LiH} + 1.5x\text{H}_2 + (1 - 0.5x)\text{Mg}$$

In addition, partial reversibility of Li–Mg–B–H has been demonstrated and 5.3 wt% hydrogen can be released in the second cycle. According to the experimental results of this work, the strategy of altering the $\chi_p$ of metal ions in $LiBH_4$ can truly improve the hydrogen storage properties of $LiBH_4$ and it may provide general guidance and inspiration in dual-cation borohydrides hydrogen storage materials with advanced and controllable performances.

## Acknowledgements

The authors gratefully acknowledge the financial supports for this research from the National Natural Science Foundation of China (51671173, 51571179 and 51471151), the Program for Innovative Research Team in University of Ministry of Education of China (IRT13037) and the Scientific Research Starting Foundation of Jiangsu University of Science and Technology (1142931607).

## References

1 M. Felderhoff, C. Weidenthaler, R. von Helmolt and U. Eberle, Hydrogen storage: the remaining scientific and technological challenges, *Phys. Chem. Chem. Phys.*, 2007, **9**, 2643–2653.
2 L. Zhang, L. Chen, X. Fan, X. Xiao, J. Zheng and X. Huang, Enhanced hydrogen storage properties of $MgH_2$ with numerous hydrogen diffusion channels provided by $Na_2Ti_3O_7$ nanotubes, *J. Mater. Chem. A*, 2017, **5**, 6178–6185.
3 L. Schlapbach and A. Züttel, Hydrogen-storage materials for mobile applications, *Nature*, 2001, **414**, 353–358.
4 A. Züttel, S. Rentsch, P. Fischer, P. Wenger, P. Sudan, P. h. Mauron and C. h. Emmenegger, Hydrogen storage properties of $LiBH_4$, *J. Alloys Compd.*, 2003, **356**, 515–520.
5 C. Luo, H. Wang, T. Sun and M. Zhu, Enhanced dehydrogenation properties of $LiBH_4$ compositing with hydrogenated magnesium-rare earth compounds, *Int. J. Hydrogen Energy*, 2012, **37**, 13446–13455.
6 Y. Zhao, Y. Liu, H. Liu, H. Kang, K. Cao, Q. Wang, C. Zhang, Y. Wang, H. Yuan and L. Jiao, Improved dehydrogenation performance of $LiBH_4$ by 3D hierarchical flower-like $MoS_2$ spheres additives, *J. Power Sources*, 2015, **300**, 358–364.
7 H. Liu, L. Jiao, Y. Zhao, K. Cao, Y. Liu, Y. Wang and H. Yuan, Improved dehydrogenation performance of $LiBH_4$ by confinement into porous $TiO_2$ micro-tubes, *J. Mater. Chem. A*, 2014, **2**, 9244–9250.
8 O. Friedrichs, J. W. Kim, A. Remhof, F. Buchter, A. Borgschulte, D. Wallachr, Y. W. Cho, M. Fichtner, K. H. Oh and A. Züttel, The effect of Al on the hydrogen sorption mechanism of $LiBH_4$, *Phys. Chem. Chem. Phys.*, 2009, **11**, 1515–1520.
9 G. Xia, Y. Guo, Z. Wu and X. Yu, Enhanced hydrogen storage performance of $LiBH_4$–Ni composite, *J. Alloys Compd.*, 2009, **479**, 545–548.
10 Y. Guo, X. Yu, L. Gao, G. Xia, Z. Guo and H. Liu, Significantly improved dehydrogenation of $LiBH_4$ destabilized by $TiF_3$, *Energy Environ. Sci.*, 2010, **3**, 465–470.
11 W. Cai, H. Wang, D. Sun and M. Zhu, Nanosize-controlled reversibility for a destabilizing reaction in the $LiBH_4$–$NaH_{2+x}$ system, *J. Phys. Chem. C*, 2013, **117**, 9566–9572.
12 P. Mauron, M. Bielmann, A. Remhof, A. Züttel, J. H. Shim and Y. W. Cho, Stability of the $LiBH_4/CeH_2$ composite system determined by dynamic PCT measurements, *J. Phys. Chem. C*, 2010, **114**, 16801–16805.
13 F. C. Gennari, L. F. Albanesi, J. A. Puszkiel and P. A. Larochette, Reversible hydrogen storage from $6LiBH_4$–$MCl_3$ (M = Ce, Gd) composites by in situ formation of $MH_2$, *Int. J. Hydrogen Energy*, 2011, **36**, 563–570.
14 F. E. Pinkerton and M. S. Meyer, Reversible hydrogen storage in the lithium borohydride-calcium hydride coupled system, *J. Alloys Compd.*, 2008, **464**, L1–L4.

15 J. J. Vajo, W. Li and P. Liu, Thermodynamic and kinetic destabilization in $LiBH_4/Mg_2NiH_4$: promise for borohydride based hydrogen storage, *Chem. Commun.*, 2010, **46**, 6687–6689.

16 D. Liu, Q. Liu, T. Si, Q. Zhang, F. Fang, D. Sun, L. Ouyang and M. Zhu, Superior hydrogen storage properties of $LiBH_4$ catalyzed by $Mg(AlH_4)_2$, *Chem. Commun.*, 2011, **47**, 5741–5743.

17 A. Surrey, C. B. Minella, N. Fechler, M. Antonietti, H. J. Grafe and L. Schultz, Improved hydrogen storage properties of $LiBH_4$ via nanoconfinement in micro- and mesoporous aerogel-like carbon, *Int. J. Hydrogen Energy*, 2016, **41**, 5540–5548.

18 P. Negen, P. Adelhelm, A. M. Beale, K. P. de Jong and P. E. de Jong, $LiBH_4$/SBA-15 nanocomposites prepared by melt infiltration under hydrogen pressure: synthesis and hydrogen sorption properties, *J. Phys. Chem. C*, 2010, **114**, 6163–6168.

19 P. Javadian, D. A. Sheppard, C. E. Buckley and T. R. Jensen, Hydrogen storage properties of nanoconfined $LiBH_4$–$Ca(BH_4)_2$, *Nano Energy*, 2015, **11**, 96–103.

20 P. Choudhury, S. S. Srinivasan, V. R. Bhethanabotla, Y. Goswami, K. McGrath and E. K. Stefanakos, Nano-Ni doped Li–Mn–B–H system as a new hydrogen storage candidate, *Int. J. Hydrogen Energy*, 2009, **34**, 6325–6334.

21 B. Zhai, X. Xiao, W. Lin, X. Huang, X. Fan, S. Li, H. Ge, Q. Wang and L. Chen, Enhanced hydrogen desorption properties of $LiBH_4$–$Ca(BH_4)_2$ by synergetic effect of nanoconfinement and catalysis, *Int. J. Hydrogen Energy*, 2016, **41**, 17462–17470.

22 J. Y. Lee, D. Ravnsbæk, Y. S. Lee, Y. Kim, Y. Cerenius, J. H. Shim, T. R. Jensen, N. H. Hur and Y. W. Cho, Decomposition reactions and reversibility of the $LiBH_4$–$Ca(BH_4)_2$ composite, *J. Phys. Chem. C*, 2009, **113**, 15080–15086.

23 Y. Zhang, Q. Tan, H. Chu, J. Zhang, L. Sun and Z. Wen, Hydrogen de/resorption properties of the $LiBH_4$–$MgH_2$–Al system, *J. Phys. Chem. C*, 2009, **113**, 21964–21969.

24 P. Ngene, M. van Zwienen and P. E. de Jongh, Reversibility of the hydrogen desorption from $LiBH_4$: a synergetic effect of nanoconfinement and Ni addition, *Chem. Commun.*, 2010, **46**, 8201–8203.

25 Z. Zhao-Karger, R. Witter, E. G. Bardaji, D. Wang, D. Cossement and M. Fichtner, Altered reaction pathways of eutectic $LiBH_4$–$Mg(BH_4)_2$ by nanoconfinement, *J. Mater. Chem. A*, 2013, **1**, 3379–3386.

26 P. Choudhury, S. S. Srinivasan, V. R. Bhethanabotla, Y. Goswami, K. McGrath and E. K. Stefanakos, Nano-Ni doped Li–Mn–B–H system as a new hydrogen storage candidate, *Int. J. Hydrogen Energy*, 2009, **34**, 6325–6334.

27 H. W. Li, S. Orimo, Y. Nakamori, K. Miwa, N. Ohba, S. Towata and A. Züttel, Materials designing of metal borohydrides: Viewpoints from thermodynamical stabilities, *J. Alloys Compd.*, 2007, **446**, 315–318.

28 Y. Nakamori, K. Miwa, A. Ninomiya, H. W. Li, N. Ohba, S. Towata, A. Züttel and S. Orimo, Thermodynamical stabilities of metal-borohydrides, *Phys. Rev. B*, 2006, **74**, 045126.

29 K. Jiang, X. Xiao, S. Deng, M. Zhang, S. Li, H. Ge and L. Chen, A Novel Li–Ca–B–H Complex Borohydride: Its Synthesis and Hydrogen Storage Properties, *J. Phys. Chem. C*, 2011, **115**, 19986–19993.

30 C. Kim, S. Hwang, R. C. Bowman Jr, J. W. Reiter, J. A. Zan, J. G. Kulleck, H. Kabbour, E. H. Majzoub and V. Ozolins, $LiSc(BH_4)_4$ as a hydrogen storage material: multinuclear high-Resolution solid-state NMR and first-Principles Density functional Theory Studies, *J. Phys. Chem. C*, 2009, **113**, 9956–9968.

31 Z. Fang, X. Kang, P. Wang, H. Li and S. I. Orimo, Unexpected dehydrogenation behavior of $LiBH_4/Mg(BH_4)_2$ mixture associated with the in situ formation of dual-cation borohydride, *J. Alloys Compd.*, 2010, **491**, L1–L4.

32 E. G. Bardají, Z. Zhao-Karger, N. Boucharat, A. Nale, M. J. van Setten, W. Lohstroh, E. Röhm, M. Catti and M. Fichtner, $LiBH_4$–$Mg(BH_4)_2$: a physical mixture of metal borohydrides as hydrogen storage material, *J. Phys. Chem. C*, 2011, **115**, 6095–6101.

33 G. L. Soloveichik, M. Andrus, Y. Gao, J. Zhao and S. Kniajanski, Magnesium borohydride as a hydrogen storage material: synthesis of unsolvated $Mg(BH_4)_2$, *Int. J. Hydrogen Energy*, 2009, **34**, 2144–2152.

34 K. Chłopek, C. Frommen, A. Léon, O. Zabara and M. Fichtner, Synthesis and properties of magnesium tetrahydroborate, $Mg(BH_4)_2$, *J. Mater. Chem.*, 2007, **17**, 3496–3503.

35 H. Kou, X. Xiao, L. Chen, S. Li and Q. Wang, Formation mechanism of $MgB_2$ in $2LiBH_4 + MgH_2$ system for reversible hydrogen storage, *Trans. Nonferrous Met. Soc. China*, 2011, **21**, 1040–1046.